Crystal structures and magnetic properties of two octacyanometalate-based tungstate(v)–copper(ii) bimetallic assemblies†

Dong-feng Li,[a] Song Gao,[b] Li-min Zheng,[a] Kai-bei Yu[c] and Wen-xia Tang*[a]

[a] *State Key Laboratory of Coordination Chemistry, Nanjing University, Nanjing 210093, China. E-mail: wxtang@netra.nju.edu.cn*
[b] *State Key Laboratory of Rare Earth Materials Chemistry andApplications, Peking University, Beijing 100871, China*
[c] *Analysis Center, Chengdu Branch of Chinese Academy of Sciences, Chengdu 610041, China*

Received (in Montpellier, France) 20th November 2001, Accepted 12th April 2002
First published as an Advance Article on the web 16th August 2002

Two novel cyanide-bridged bimetallic assemblies based on octacyanotungstate as the building block, $[Cu(tn)_2]_2[W(CN)_8](OH)\cdot H_2O$ (**1**) and $\{[Cu(dien)]_2[W(CN)_8](OH)\cdot 3H_2O\}_\infty$ (**2**) (tn = 1,3-diaminopropane; dien = diethylenetriamine), have been prepared and their magnetic properties studied. The X-ray analysis shows that the structure of **1** consists of a trinuclear unit, $Cu(tn)_2$–N–C–$W(CN)_6$–C–N–$Cu(tn)_2$, which acts as a basic component that is connected through weak axial Cu···N–C–W interactions to form a two-dimensional sheet network. In the structure of **2**, each $W(CN)_8$ fragment connects four Cu(dien) groups through two types of W–C–N–Cu linkages in a $-(A-B)_n-$ pattern along the diagonal lines of the *a* and *b* axes to form an infinite 2-D layer structure. Magnetic susceptibility data demonstrate that the magnetic behavior of both **1** and **2** is characteristic of ferromagnetic interactions onto which weak antiferromagnetic interactions are superimposed.

Over the past decade hexacyanometalates $M(CN)_6^{n-}$ (M = Fe, Cr, Mn, *etc.*) acting as building blocks have been utilized extensively to: (*i*) obtain molecular-based magnetic materials exhibiting spontaneous magnetization and (*ii*) explore the relationship between structure and magnetism.[1–30] As a result of the research ardor in this area, significance progress has been achieved, and the strategies and methods obtained in the research process will cast light on the study of molecule-based magnetic materials in the future.

Recently, the paramagnetic anions $M^v(CN)_8^{3-}$ (M = Mo, W) have attracted much attention.[31–33] Compared with the octahedral hexacyanometalate species $M(CN)_6^{n-}$, the octacyanometalates $M^v(CN)_8^{3-}$ may show various geometrical structures (*e.g.*, square antiprism, dodecahedron, bicapped trigonal prism), depending on the external environment.[33,34] These species may be used as versatile supramolecular synthons to construct a variety of supramolecular architectures or networks with novel topological structures. The diversity of structures may lead to various magnetic features which is just one of the aims of the magnetostructural studies. Nevertheless, only a few bimetallic assemblies based on $[M^v(CN)_8]^{3-}$ have been studied structurally and magnetically so far, which have shown intriguing magnetic properties.[31–33] For instance, $\{Mn^{II}_9[Mo^v(CN)_8]_6\cdot 24CH_3OH\}\cdot 5CH_3OH\cdot 2H_2O$[32] is the highest ground-state molecular cluster ($S = 51/2$) to date. It is worth noting that a Cu^{II}–Mo^{IV} bimetallic cyanide-bridged compound reported by Rombaut *et al.* shows reversible photomagnetic effects and can act as a switchable molecular spin device.[35] However, given the limited number of examples of octacyanometalate magnetic species, it is still unclear how to describe the relationship between magnetism and structure for octacyanometalate cyano-bridged bimetallic compounds. With the hope of gaining insight into the magnetostructural correlation and to seek new molecular-based magnetic materials, we have initiated a study on bimetallic assemblies comprised of $[W^v(CN)_8]^{3-}$ and unsaturated transition metal coordination complexes. Here, we report the structures and magnetic properties of two novel Cu(ii)–W(v) cyano-bridged bimetallic compounds, $[Cu(tn)_2]_2[W(CN)_8](OH)\cdot H_2O$ (**1**) and $\{[Cu(dien)]_2[W(CN)_8](OH)\cdot 3H_2O\}_\infty$ (**2**) (tn = 1,3-diaminopropane; dien = diethylenetriamine).

Experimental

Measurements

The samples for C, H and N analyses were dried in vacuum and the analyses were made on a Perkin–Elmer 240C elemental analyzer. Infrared spectra were measured on a Bruker Vector 22 FT-IR instrument from KBr pellets. The magnetic susceptibilities and field dependence of magnetization up to 5 T at 1.8 K were obtained on polycrystalline samples using a Model MagLab System 2000 magnetometer. The experimental susceptibilities were corrected for the sample holder and the diamagnetism contributions estimated from Pascal's constants. Effective magnetic moments were calculated using the equation $\mu_{eff} = 2.828(\chi_M T)^{1/2}$, where χ_M is the molar magnetic susceptibility.

Preparations

All chemicals and reagents were used as received. $K_3[W(CN)_8]\cdot H_2O$ was prepared according to published procedures.[36]

$[Cu(tn)_2]_2[W(CN)_8](OH)\cdot H_2O$ (1). To an aqueous solution (20 cm^3) of $Cu(ClO_4)_2\cdot 6H_2O$ (148.2 mg, 0.4 mmol) and excess 1,3-diaminopropane (tn; 0.05 ml, 1.2 mmol), $K_3[W(CN)_8]\cdot H_2O$

† Electronic supplementary information (ESI) available: ORTEP drawing of the asymmetric unit for **2**; packing diagrams for **1** and **2**; temperature dependence of χ_M^{-1} for **1**; field dependence of the magnetization for **2**; temperature dependence of the magnetization with ZFCM and FCM for **1** and **2**, respectively. See http://www.rsc.org/suppdata/nj/b1/b110635j/

 DOI: 10.1039/b110635j

(105.5 mg, 0.2 mmol) in 20 cm^3 distilled water was added with stirring at room temperature. The resulting deep blue solution (pH *ca.* 9) was allowed to stand for several days and dark blue rod-like crystals were obtained. They were collected by suction filtration, washed with water, and dried in air. All the operations for the synthesis were carried out in the dark to avoid decomposition of $K_3[W(CN)_8]\cdot H_2O$. Yield: 112 mg (66%). Anal. calcd. for $C_{20}H_{43}N_{16}O_2Cu_2W$: C, 28.24; H, 5.10; N, 26.35%. Found: C, 28.25; H, 5.12; N, 26.33%. IR (cm^{-1}, KBr disk): $\nu_{C\equiv N}$ 2093 (vs), 2101 (s), 2131 (m).

$\{[Cu(dien)]_2[W(CN)_8](OH)\cdot 3H_2O\}_\infty$ (2). This assembly was prepared as dark blue crystals in a way similar to that of **1**, except for the use of excess diethylenetriamine (dien; 0.09 ml, 0.8 mmol) instead of tn. Yield: 88 mg (55%). Anal. calcd. for $C_{16}H_{33}N_{14}O_4Cu_2W$: C, 24.13; H, 4.18; N, 24.62%. Found: C, 24.05; H, 4.26; N, 24.72%. IR (cm^{-1}, KBr disk): $\nu_{C\equiv N}$ 2112 (s), 2158 (m).

Caution! Perchlorate salts of compounds containing organic ligands are potentially explosive, especially when heated or bumped. Only small quantities of these compounds should be prepared and handled behind suitable protective shields.

X-Ray crystallography

Intensity data for the crystals of **1** and **2** were collected on a Siemens Apex SMART CCD system equipped with monochromated Mo-Kα radiation ($\lambda = 0.71073$ Å) at room temperature. The data integration and empirical absorption corrections were carried out by SAINT[37] and SADABS[38] programs, respectively. The structures were solved by direct methods and refined on F^2 using the SHELXTL suite of program.[39] For **1**, all non-hydrogen atoms were refined anisotropically by full-matrix least-squares methods. The C–H and N–H hydrogen atoms were computed and refined isotropically using a riding model. The hydrogen atoms of the water molecule O1 were found from ΔF maps. To balance the charge and considering the symmetry, the S.O.F. of the two hydrogen atoms on O1 in the asymmetric unit were averagely fixed at 0.75. The largest difference peak and hole were 2.942 and -2.053 e·Å^{-3}, respectively, and were within 0.90 Å from W1. For **2**, except for the disordered atoms of dien (C5, C6, C7 and C8, S.O.F. 0.5), all other non-hydrogen atoms were refined anisotropically. Hydrogen atoms were generated geometrically. The hydrogen atoms of water molecules O1W and O2W were not added. Considering the charge balance and symmetry, O1W and O2W will share 3.5 hydrogen atoms statistically. Crystal and refinement data for **1** and **2** are listed in Table 1.

Table 1 Crystal data for complex $[Cu(tn)_2]_2[W(CN)_8](OH)\cdot H_2O$, **1**, and $\{[Cu(dien)]_2[W(CN)_8](OH)\cdot 3H_2O\}_\infty$, **2**

	1	**2**
Formula	$C_{20}H_{43}N_{16}O_2Cu_2W$	$C_{16}H_{33}N_{14}O_4Cu_2W$
Formula weight	850.63	796.49
Crystal system	Monoclinic	Orthorhombic
Temperature/K	293	293
Space group	$C2/c$	$P2_12_12$
a/Å	15.757(3)	12.869(3)
b/Å	10.903(2)	9.953(3)
c/Å	19.365(4)	11.375(3)
β/°	110.46(3)	90.00
Z	4	2
μ/mm^{-1}	5.082	5.432
Reflections collected/unique	7397/2508	7653/2572
R_{int}	0.0453	0.0704
R_1 [$I > 2\sigma(I)$]	0.0398	0.0381
wR_2 [$I > 2\sigma(I)$]	0.0992	0.0620
R_1 (all data)	0.0444	0.0446
wR_2 (all data)	0.1013	0.0630

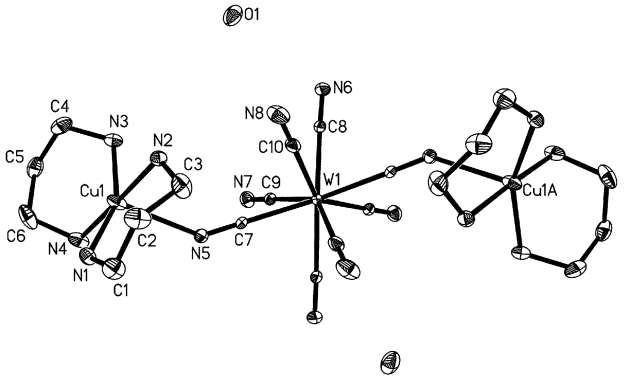

Fig. 1 ORTEP drawing for $[Cu(tn)_2]_2[W(CN)_8](OH)\cdot H_2O$ (**1**); symmetry code: $-x+3/2$, $y-1/2$, $-z+1/2$. Hydrogen atoms are omitted for clarity.

CCDC reference numbers 174519–174520. See http://www.rsc.org/suppdata/nj/b1/b110635j/ for crystallographic data in CIF or other electronic format.

Results and discussion

Structures

$[Cu(tn)_2]_2[W(CN)_8](OH)\cdot H_2O$, 1. The compound crystallizes in the $C2/c$ space group, and contains one copper site and half a W atom localized at the special equivalent positions. An ORTEP drawing of $[Cu(tn)_2]_2[W(CN)_8](OH)\cdot H_2O$ is shown in Fig. 1. It consists of one octacyanotungstate $W(CN)_8$ fragment coordinated *via* two cyano bridges to two $Cu(tn)_2$ fragments, the six other cyano groups being terminal. The W atom is coordinated by eight CN groups in an irregular square antiprism with W–C distances ranging from 2.146(7) to 2.163(7) Å. The Cu coordination sphere can be described as a distorted square pyramidal geometry with the equatorial coordinated atoms N1, N2, N3, N4 and the axial atom N5. The former four nitrogen atoms are from two tn ligands with $Cu–N_{eq}$ distances ranging from 1.991(6) to 2.042(6) Å, while N5 is from a cyano group of the $W(CN)_8$ fragment with a longer $Cu–N_{ax}$ distance of 2.421(6) Å. The W–C–N angles are almost linear, ranging from 177.6(6)° to 178.9(6)°, whereas Cu1–N5–C7 deviates from linearity with an angle of 141.8(5)° (see Table 2). The intramolecular distances W1···Cu1

Table 2 Selected bond distances (Å) and angles (°) for $[Cu(tn)_2]_2[W(CN)_8](OH)\cdot H_2O$, **1**

Cu1–N1	2.011(6)	Cu1–N4	2.016(6)
Cu1–N2	1.991(6)	Cu1–N5	2.421(6)
Cu1–N3	2.042(6)	Cu1^a–N6	3.102(7)
W1–C7	2.163(7)	W1–C9	2.157(7)
W1–C8	2.146(7)	W1–C10	2.158(8)
N5–C7	1.133(8)	N7–C9	1.142(9)
N6–C8	1.155(8)	N8–C10	1.137(10)
N5–C7–W1	178.9(6)	N7–C9–W1	178.7(7)
N6–C8–W1	177.6(6)	N8–C10–W1	178.7(8)
C7–W1–C7^b	141.6(3)	C1–N1–Cu1	124.4(5)
N2–Cu1–N4	176.3(3)	N1–Cu1–N5	105.9(2)
N2–Cu1–N1	93.3(2)	N3–Cu1–N5	98.0(2)
N4–Cu1–N1	90.3(3)	N4–Cu1–N5	92.5(3)
N2–Cu1–N3	91.4(3)	C3–N2–Cu1	118.8(5)
N4–Cu1–N3	85.0(3)	C4–N3–Cu1	116.3(5)
N1–Cu1–N3	155.8(3)	C6–N4–Cu1	113.0(6)
N2–Cu1–N5	87.1(2)	C7–N5–Cu1	141.8(5)

Symmetry operations: ^{a} $-x+1/2$, $y+1/2$, $-z+1/2$; ^{b} $-x+1$, y, $-z+1/2$.

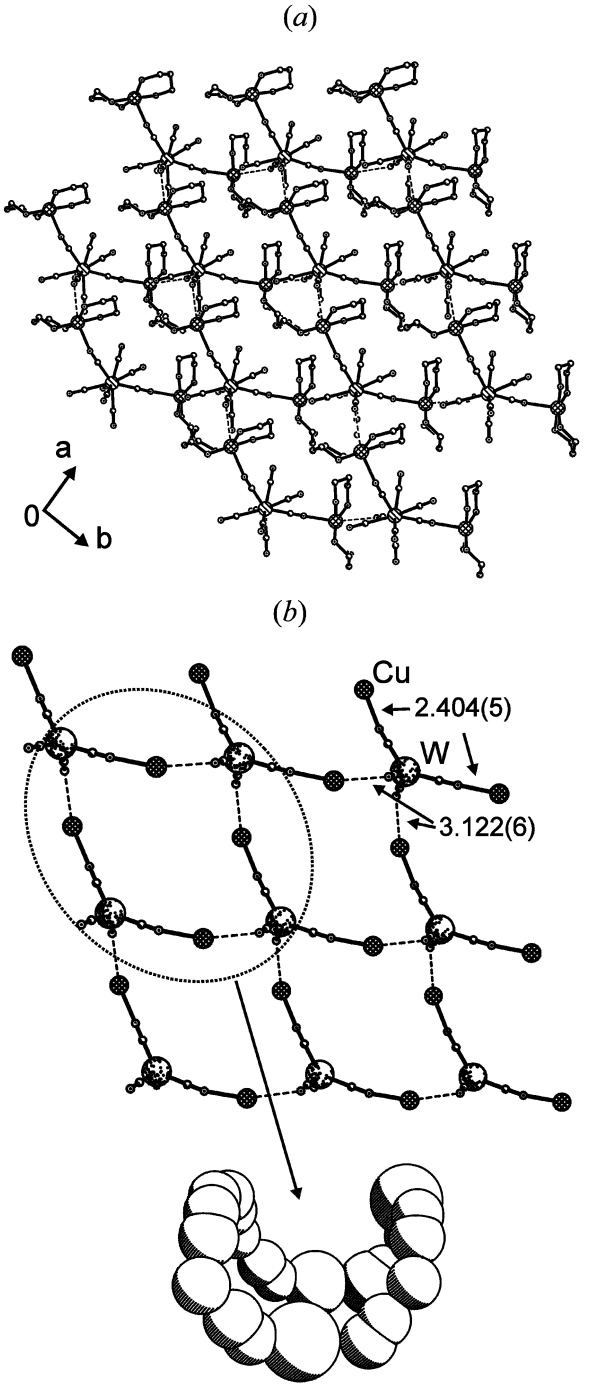

Fig. 2 (*a*) Projection of the layer structure of **1** along the *c* axis. (*b*) The backbone structure of this layer and the $W_4Cu_4(CN)_8$ 24-atom macrocyclic unit with a saddle-shape structure.

(or Cu1A), and Cu1···Cu1A are equal to 5.411(2) and 9.851(4) Å, respectively, with an angle Cu1–W1–Cu1A of 131.1(1)°. Fig. 2(a) shows the layer structure of **1** along the *c* axis and Fig. 2(b) shows the backbone structure of this layer. It can be seen that each Cu_2W trinuclear unit links two adjacent such trinuclear units through two cyano groups (C8–N6 and C8A–N6A), forming weak Cu···N interactions with a long Cu···$N_{cyanide}$ distance, $Cu1^a$–N6 = 3.102(7) Å, owing to the Jahn–Teller effect,[27] thus constructing a 2-D sheet structure. The water molecules and OH^- groups are situated within the 2-D layers and hydrogen-bonded to the terminal CN groups and the nitrogen atoms of the tn ligand with O···N distances ranging from 2.806(12) to 3.102(9) Å. In addition, from the projective figure of the layer, there is a $W_4Cu_4(CN)_8$ 24-atom macrocyclic grid-like unit. However, these atoms are far from planar, instead forming a saddle-shape structure [see Fig. 2(b)].

$\{[Cu(dien)]_2[W(CN)_8](OH)\cdot 3H_2O\}_\infty$, 2. The perspective view of a segment of **2** along the *c* axis with the atom-numbering scheme is given in Fig. 3, which shows five trinuclear $(Cu_2W)_5$ units bridged by CN groups extending along the diagonal directions of the *a* and *b* axes. Similar to the case of **1**, the basic unit contains one copper site and half a W atom localized at the special equivalent positions (see Fig. S1 in the Electronic supplementary information, ESI). The W atom is coordinated by eight CN groups in a distorted square antiprism with W–C distances ranging from 2.114(9) to 2.170(10) Å. The coordination environment around Cu1 can be described as a distorted square pyramidal geometry with the equatorial coordinated atoms N1, N5, N6, N7 and the apical atom N2B from the adjacent $W(CN)_8$ fragment. The nitrogen atoms N5, N6A (or N6B) and N7 are from the dien ligand with Cu–N_{eq} distances ranging from 2.00(2) to 2.031(10) Å, while N1 is from a cyano group with a Cu–N_{eq} distance of 1.959(8) Å. The W–C–N angles deviate slightly from linearity with angles ranging from 175.1(9) to 178.9(7)°, whereas Cu1–N1–C1 and Cu1D–N2–C2 angles are 160.8(9)° and 140.8(7)°, respectively. The octacyanotungstate $W(CN)_8$ fragment coordinates to two Cu(dien) fragments, *via* two cyano bridges (C1–N1 and C1A–N1A) with a short Cu–N_{CN} distance of 1.959(8) Å along the diagonal of the *a* and *b* axes, while it can also link the two other Cu(dien) fragments along the other diagonal of the *a* and *b* axes, *via* two cyano bridges (C2–N2 and C2A–N2A) with a longer Cu–N_{CN} distance, Cu1D–N2 = 2.313(8) Å (Table 3). As a result, an infinite two-dimensional sheet structure is formed through the two types of W–CN–Cu linkages in a $-(A-B)_n-$ pattern along the diagonal directions of the *a* and *b* axes. Fig. 4 shows the projection of the 2-D layer structure on the *ab* plane. Similar to complex **1**, the 2-D layer also contains 24-atom macrocyclic $[Cu_4W_4(CN)_8]$ structures with irregular polygons. The water molecules and OH^- counteranions are located between the sheets and hydrogen-bonded to the terminal CN ligand of $W(CN)_8^{3-}$ and the coordinating dien ligand with O···N distances ranging from 2.994(11) to 3.258(13) Å; the resulting hydrogen bonds link the adjacent layers to form a 3-D network (see Fig. S2 in ESI). The intramolecular distances W1···Cu1 (or Cu1A), W1···Cu1D (or Cu1G), Cu1···Cu1A and Cu1D···Cu1G are equal to 5.142(2), 5.261(2), 5.925(3) and 10.507(3) Å, respectively, with

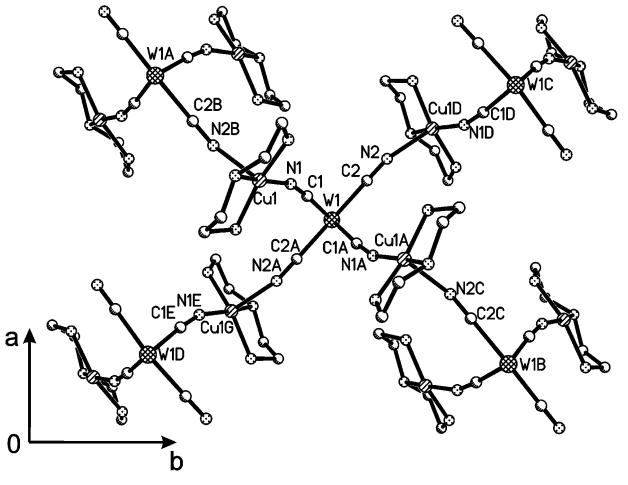

Fig. 3 Projection of a five-trinuclear fragment $(Cu_2W)_5$ along the *c* axis for **2** with the atom-labeling scheme. Hydrogen atoms, C and N atoms of the non-bridged cyanides are omitted for clarity.

Table 3 Selected bond distances (Å) and angles (°) for $\{[Cu(dien)]_2[W(CN)_8](OH)\cdot 3H_2O\}_\infty$, **2**

Cu1–N1	1.959(8)	Cu1–N7	2.031(10)
Cu1D[a]–N2	2.313(8)	Cu1–N6A	2.00(2)
Cu1–N5	2.017(10)	Cu1–N6B	2.02(4)
W1–C1	2.114(9)	W1–C3	2.153(8)
W1–C2	2.122(9)	W1–C4	2.170(10)
C1–N1	1.163(10)	C3–N3	1.166(10)
C2–N2	1.161(10)	C4–N4	1.167(10)
N1–C1–W1	175.1(9)	N3–C3–W1	178.9(7)
N2–C2–W1	178.1(8)	N4–C4–W1	176.1(9)
C2–N2–Cu1D[a]	140.8(7)	C1–N1–Cu1	160.8(9)
N1–Cu1–N5	93.3(4)	N7–Cu1–N6A	76.4(7)
N1–Cu1–N7	95.5(4)	N1–Cu1–N2[b]	99.7(3)
N5–Cu1–N7	161.5(4)	N5–Cu1–N2[b]	96.0(4)
N1–Cu1–N6B	165.7(9)	N7–Cu1–N2[b]	98.5(3)
N5–Cu1–N6B	74.9(8)	N6B–Cu1–N2[b]	89.7(12)
N7–Cu1–N6B	93.8(9)	N6A–Cu1–N2[b]	89.5(9)
N1–Cu1–N6A	168.6(8)	C8B–N7–Cu1	98.2(10)
N5–Cu1–N6A	92.5(7)	C7A–N6A–Cu1	107.5(15)
C5B–N5–Cu1	115.8(12)	C6A–N6A–Cu1	107.0(16)
C5A–N5–Cu1	99.1(13)	C6B–N6B–Cu1	114.0(3)
C8A–N7–Cu1	122.8(12)	C7B–N6B–Cu1	99.1(19)

Symmetry operations: [a] $x+1/2, -y+5/2, -z+1$; [b] $x-1/2, -y+5/2, -z+1$.

Cu1–W1–Cu1A and Cu1D–W1–Cu1G angles of 70.36(3)° and 173.83(3)° (Fig. 3).

Magnetic properties

Compound 1. The variable temperature magnetic susceptibility data for complex **1** was recorded between 2–300 K under a magnetic field of 10 kOe. The plots of $\chi_M T$ *vs.* T and χ_M *vs.* T are shown in Fig. 5. At room temperature, $\chi_M T$ is equal to 1.03 $cm^3\ mol^{-1}$ K (2.87 μ_B) per Cu_2W unit, which closely approximates the predicted spin-only value (1.125 $cm^3\ mol^{-1}$ K, 3.00 μ_B per Cu_2W) for two Cu(II) ($S = 1/2$) and a W(V) ($S = 1/2$) centers ($g = 2.0$). As the temperature is lowered, the $\chi_M T$ value steady increases up to a maximum value of 1.19 $cm^3\ mol^{-1}$ K around 30 K, which suggests the presence of ferromagnetic exchange between the neighboring Cu and W ions. In accord with this, the plot of $1/\chi_M$ *vs.* T (see Fig. S3 in ESI†) above 30 K obeys the Curie–Weiss law with a positive Weiss constant $\theta = +8.1$ K. Below 30 K, $\chi_M T$ decreases abruptly down to 2 K (0.93 $cm^3\ mol^{-1}$ K), indicating the existence of an antiferromagnetic coupling among the adjacent trinuclear Cu_2W units at low temperature.

The field dependence of magnetization for **1** measured at 1.8 K is shown in the inset in Fig. 5. It can be seen that the observed magnetization (per Cu_2W) is smaller than the value predicted from the Brillouin function for two Cu(II) ions and a W(V) ion with $g = 2.0$; and the magnetization per Cu_2W at 50 kOe is 2.61 μ_B, slightly smaller than the expected saturation value of 3.0 μ_B for two Cu(II) ions and a W(V) ion. This implies that an antiferromagnetic interaction among the adjacent trinuclear Cu_2W units has a major effect in such a situation at 1.8 K, which is agreement with the magnetic susceptibility result that the antiferromagnetic coupling among the adjacent trinuclear Cu_2W units plays a primary role at low temperature.

Furthermore, if we ignore the weak axial $Cu\cdots N_{cyanide}$ interactions among the trinuclear Cu_2W units [see Fig. 2(b)], we can interpret the magnetic behavior of **1** through a trinuclear model (1/2–1/2–1/2) with the spin Hamiltonian: $\hat{H} = -2J(\hat{S}_{Cu1}\hat{S}_{W1} + \hat{S}_{Cu1A}\hat{S}_{W1})$. Considering the underlying temperature-independent paramagnetism of the Cu(II) and W(V) ions and a variable monomeric impurity level, the molar susceptibility is given as:

$$\chi = (1-p)\frac{Ng^2\beta^2}{4kT} \times \frac{10 + \exp(-J/kT) + \exp(-3J/kT)}{2 + \exp(-J/kT) + \exp(-3J/kT)} + p\frac{Ng^2\beta^2 S(S+1)}{kT} + \chi_{TIP} \quad (1)$$

where N, k and β are Avogadro's number, Boltzmann's constant and Bohr magneton, respectively, p is the mole percentage of paramagnetic impurity, and χ_{TIP} is the temperature-independent paramagnetism. Considering the further interaction between the magnetic units, the formula of the

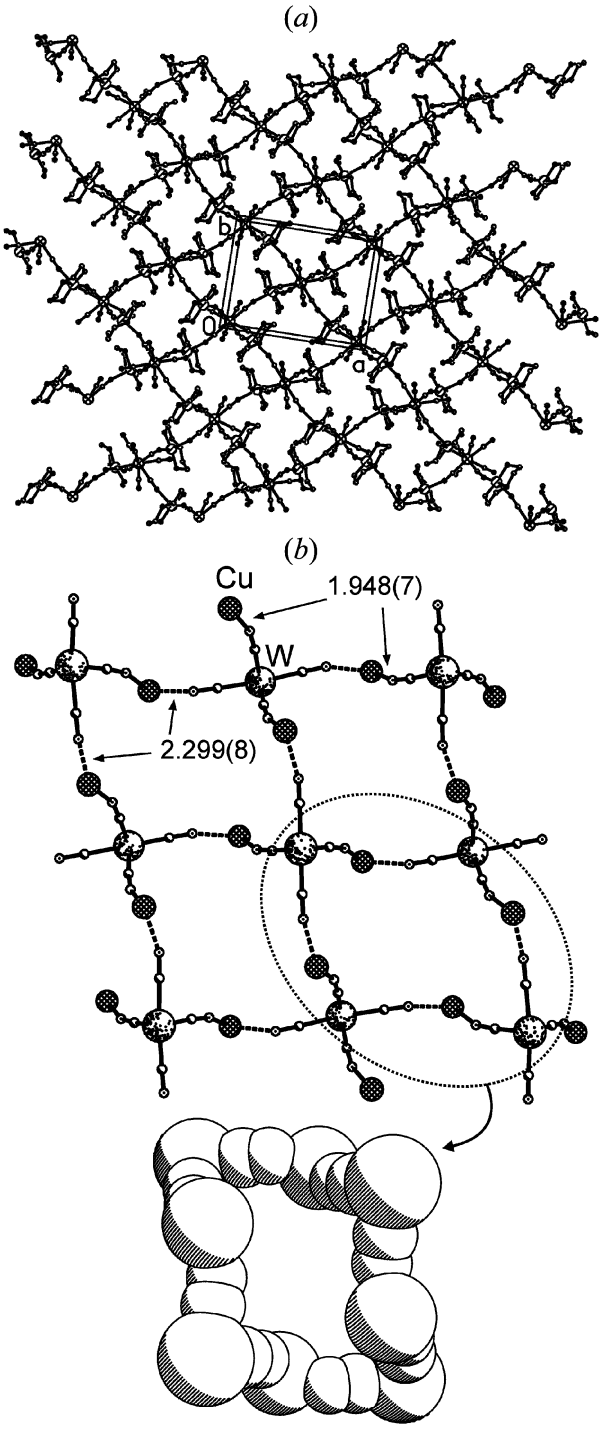

Fig. 4 Projection of (*a*) the infinite 2-D layer structure and (*b*) the backbone structure of this layer on the *ab* plane and the $W_4Cu_4(CN)_8$ 24-atom macrocyclic unit for **2**.

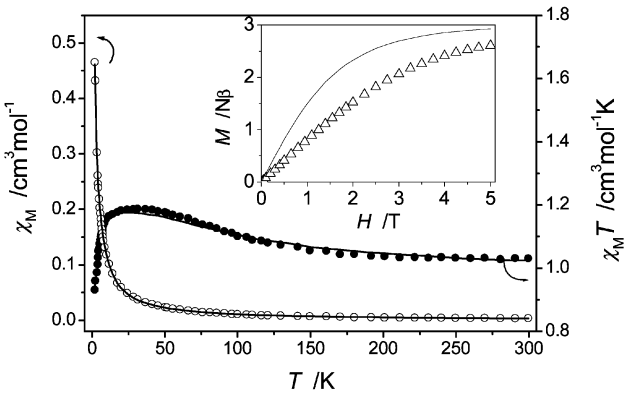

Fig. 5 Plot of the temperature dependence of $\chi_M T$ (●) and χ_M (○) for complex **1** (per Cu_2W). The solid line represents the best theoretical fit (see text). Inset: field dependence of the magnetization M (Δ) for **1** at 1.8 K.

factual susceptibility can be modified by molecular field theory as follows:[40]

$$\chi_M = \frac{\chi}{1 - 4zJ'\chi/Ng^2\beta^2} \quad (2)$$

Assuming the same g values, the best fit for $\chi_M T$ *vs.* T in the range of 2–300 K (solid line shown in Fig. 5 leads to the following parameters: $J = 3.57$ cm^{-1}, $J' = -0.14$ cm^{-1} (for $z = 4$), $g = 1.99$, $p = 2.14 \times 10^{-3}$, $\chi_{TIP} = 1.42 \times 10^{-4}$ cm^3 mol^{-1} and $R = 3.69 \times 10^{-3}$ $\{R = \sum[(\chi_M)_{obs} - (\chi_M)_{calcd}]^2/\sum[(\chi_M)_{obs}]^2\}$. J represents the interaction between W1···Cu1 (or W1···Cu1A) through the cyanide bridge, the positive value demonstrates the presence of ferromagnetic coupling within the Cu_2W units; while the negative value for J' implies that weak antiferromagnetic exchange interactions occur among the adjacent Cu_2W magnetic units.

Compound 2. The variable temperature magnetic susceptibility data was measured between 4–300 K under a magnetic field of 5 kOe. The plot of $\chi_M T$ *vs.* T is shown in Fig. 6, which also reveals a weak ferromagnetic coupling with antiferromagnetic interactions dominant at low temperature. Similar to complex **1**, the $\chi_M T$ value of complex **2** is equal to 1.09 cm^3 mol^{-1} K (2.95 μ_B) per Cu_2W unit at room temperature, which is very close to the expected spin-only value for two Cu(II) and a W(V) centers ($g = 2.0$). Upon cooling, the $\chi_M T$ value increases up to a maximum value of 1.19 cm^3 mol^{-1} K around 22 K. Below 22 K, $\chi_M T$ abruptly decreases to 0.94 cm^3 mol^{-1} K at 4 K. The Curie–Weiss plot in the temperature range of 30–300 K gave a positive Weiss constant $\theta = +3.7$ K (see Fig. 6). The results imply that a ferromagnetic exchange

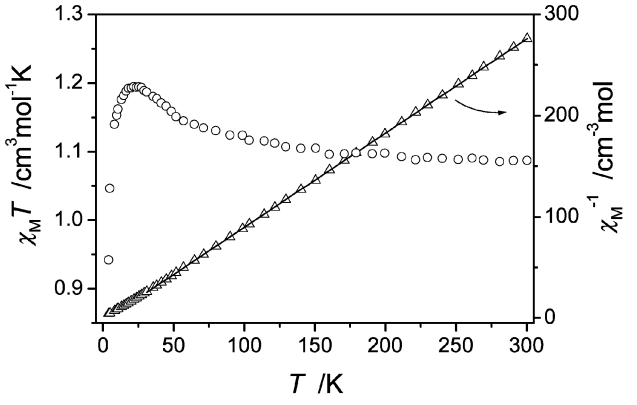

Fig. 6 Plot of the temperature dependence of $\chi_M T$ (○) and $\chi_M{}^{-1}$ (Δ) for complex **2** (per Cu_2W).

interaction exists in the 2-D layer network. The abrupt decrease in the $\chi_M T$ *vs.* T plot below 22 K may result from an inter-layer antiferromagnetic interaction. The field dependence of magnetization for **2** was measured at 1.8 K (see Fig. S4 in the ESI). Similar to **1**, the observed magnetization (per Cu_2W) is smaller than the value predicted from the Brillouin function. This indicates the presence of a dominant antiferromagnetic coupling in this complex at 1.8 K, which is consistent with the result deduced from the magnetic susceptibility data, that the inter-layer antiferromagnetic interaction is dominant at low temperature.

The origin of the ferromagnetic interaction between the Cu^{II} ($3d^9$) and W^{V} ($5d^1$) ions can be rationalized in terms of the strict orthogonality of the magnetic orbitals of these ions. According to the crystal structure and ligand-field theory, a copper(II) ion in a square pyramidal geometry has one unpaired electron in a $d_{x^2-y^2}$ orbital, which interacts with molecular orbitals of the cyano bridge having the same symmetry, producing a magnetic orbital with σ character. A tungstate(V) ion in a square antiprism environment has unpaired electron density in the d_{z^2} orbital (a^1),[41,42] which interacts with other molecular orbitals of the same cyano bridge having appropriate symmetry, producing a magnetic orbital with π character. The σ/π interaction would lead to zero overlap and thus to a strict orthogonality. Furthermore, the reason that the ferromagnetic interactions in the two complexes are very weak may be attributed to the big Cu–N–C bent angle, which will markedly weaken the ferromagnetic interaction through the W–C–N–Cu linkage.

Conclusions

In this paper, we presented the structures and preliminary magnetic studies of two novel cyanide-bridged bimetallic assemblies based on octacyanotungstate as the building block, $[Cu(tn)_2]_2[W(CN)_8](OH)\cdot H_2O$ (**1**) and $\{[Cu(dien)]_2[W(CN)_8](OH)\cdot 3H_2O\}_\infty$ (**2**). The structure analysis shows that **1** consists of a trinuclear unit, $Cu(tn)_2$–NC–$W(CN)_6$–CN–$Cu(tn)_2$, which acts as a basic moiety that is connected through weak axial Cu···$N_{cyanide}$ interactions to form a two-dimensional sheet network. In the structure of **2**, each $W(CN)_8$ fragment connects four Cu(dien) groups through two types of W–CN–Cu linkages in a–(A–B)$_n$– pattern extended along the *ab* plane to form an infinite 2-D layer structure. Magnetic susceptibility data demonstrate that the magnetic behavior of both complexes corresponds to a weak ferromagnetic coupling with a weak intermolecular antiferromagnetic interaction or interlayer antiferromagnetic interaction. The magnetic behavior of the two complexes is similar, which may be due to the similarity in structure of the two compounds [see Fig. 2(b) and 4(b)].

Acknowledgements

This work was supported by the National Natural Science Foundation of China. We thank Professor C.-y Duan and Dr. X.-m Ren from the State Key Laboratory of Coordination Chemistry, Nanjing University, for the refinement of the crystal structures and helpful discussions on magnetism, respectively.

References

1 V. Gadet, T. Mallah, I. Castro and M. Verdaguer, *J. Am. Chem. Soc.*, 1992, **114**, 9213.
2 T. Mallah, S. Thiébaut, M. Verdaguer and P. Veillet, *Science*, 1993, **262**, 1554.

3 M. Ohba, N. Maruono, H. Ōkawa, T. Enoki and J.-M. Latour, *J. Am. Chem. Soc.*, 1994, **116**, 11 566.
4 S. Ferlay, T. Mallah, R. Quahes, P. Veillet and M. Verdaguer, *Nature (London)*, 1995, **378**, 701.
5 W. R. Entley and G. S. Girolami, *Science*, 1995, **268**, 397.
6 O. Kahn, *Nature (London)*, 1995, **378**, 667.
7 H. Miyasaka, N. Matsumoto, H. Ōkawa, N. Re, E. Gallo and C. Floriani, *Angew. Chem., Int. Ed. Engl.*, 1995, **34**, 1446.
8 T. Mallah, C. Auberger, M. Verdaguer and P. Viellet, *J. Chem. Soc., Chem. Commun.*, 1995, 61.
9 M. Ohba, H. Ōkawa, T. Ito and A. Ohto, *J. Chem. Soc., Chem. Commun.*, 1995, 1545.
10 A. Scuiller, T. Mallah, M. Verdaguer, A. Nivorozkhin, J. Tholence and P. Veillet, *New J. Chem.*, 1996, **20**, 1.
11 R. J. Parker, D. C. R. Hockless, B. Moubaraki, K. S. Murray and L. Spiccia, *Chem. Commun.*, 1996, 2789.
12 O. Sato, T. Iyoda, A. Fujishima and K. Hashimoto, *Science*, 1996, **271**, 49.
13 M. Verdaguer, *Science*, 1996, **272**, 698.
14 O. Sato, T. Iyoda, A. Fujishima and K. Hashimoto, *Science*, 1996, **272**, 704.
15 H. Miyasaka, N. Matsumoto, H. Ōkawa, N. Re, E. Gallo and C. Floriani, *J. Am. Chem. Soc.*, 1996, **118**, 981.
16 M. S. El Fallah, E. Rentschler, A. Caneschi, R. Sessoli and D. Gatteschi, *Angew. Chem., Int. Ed. Engl.*, 1996, **35**, 1947.
17 N. Re, E. Gallo, C. Floriani, H. Miyasaka and N. Matsumoto, *Inorg. Chem.*, 1996, **35**, 6004.
18 D. G. Fu, J. Chen, X. S. Tan, L. J. Jiang, S. W. Zhang, P. J. Zheng and W. X. Tang, *Inorg. Chem.*, 1997, **36**, 220.
19 H. Miyasaka, N. Matsumoto, N. Re, E. Gallo and C. Floriani, *Inorg. Chem.*, 1997, **36**, 670.
20 M. Ohba, H. Ōkawa, N. Fukita and Y. Hashimoto, *J. Am. Chem. Soc.*, 1997, **119**, 1011.
21 M. Ohba, N. Fukita and H. Ōkawa, *J. Chem. Soc., Dalton Trans.*, 1997, 1733.
22 E. Dujardin, S. Ferlay, X. Phan, C. Desplanches, C. Cartier dit Moulin, P. Sainctavit, F. Baudelet, E. Dartyge, P. Veillet and M. Verdaguer, *J. Am. Chem. Soc.*, 1998, **120**, 11 347.
23 N. Fukita, M. Ohba, H. Ōkawa, K. Matsuda and H. Iwamura, *Inorg. Chem.*, 1998, **37**, 842.
24 M. Ohba, N. Usuki, N. Fukita and H. Ōkawa, *Angew. Chem., Int. Ed.*, 1999, **38**, 1795.
25 A. Marvilliers, S. Parsons, E. Rivière, J.-P. Audière and T. Mallah, *Chem. Commun.*, 1999, 2217.
26 S.-W. Zhang, D.-G. Fu, W.-Y. Sun, Z. Hu, K.-B. Yu and W.-X. Tang, *Inorg. Chem.*, 2000, **39**, 1142.
27 E. Colacio, J. M. Domínguez-Vera, M. Ghazi, R. Kivekäs, J. M. Moreno and A. Pajunen, *J. Chem. Soc., Dalton. Trans.*, 2000, 505.
28 R. J. Parker, L. Spiccia, K. J. Berry, G. D. Fallon, B. Moubaraki and K. S. Murray, *Chem. Commun.*, 2001, 333.
29 K. Inoue, H. Imai, P. S. Ghalsasi, K. Kikuchi, M. Ohba, H. Ōkawa and J. V. Yakhmi, *Angew. Chem., Int. Ed.*, 2001, **40**, 4242.
30 H.-Z. Kou, S. Gao, J. Zhang, G.-H. Wei, G. Su, R. K. Zheng and X. X. Zhang, *J. Am. Chem. Soc.*, 2001, **123**, 11 809.
31 Z. J. Zhong, H. Seino, Y. Mizobe, M. Hidai, A. Fujishima, S. Ohkoshi and K. Hashimoto, *J. Am. Chem. Soc.*, 2000, **122**, 2952.
32 J. Larionova, M. Gross, M. Pilkington, H. Andres, H. Stoeckli-Evans, H. U. Güdel and S. Decurtins, *Angew. Chem., Int. Ed.*, 2000, **39**, 1605.
33 Z. J. Zhong, H. Seino, Y. Mizobe, M. Hidai, M. Verdaguer, S. Ohkoshi and K. Hashimoto, *Inorg. Chem.*, 2000, **39**, 5095.
34 J. G. Leipoldt, S. S. Basson and A. Roodt, *Adv. Inorg. Chem.*, 1993, **32**, 241.
35 G. Rombaut, M. Verelst, S. Golhen, L. Ouahab, C. Mathoniére and O. Kahn, *Inorg. Chem.*, 2001, **40**, 1151.
36 H. Baadsgaard and W. D. Treadwell, *Helv. Chim. Acta*, 1955, **38**, 1669.
37 SAINT, ver. 4.0, Data Integration Software, Bruker AXS Inc., Madison, WI, 1997.
38 G. M. Sheldrick, SADABS, ver. 2.01, Empirical Absorption Correction Program, University of Göttingen, Germany, 1996.
39 G. M. Sheldrick, SHELXTL ver. 5.10, Program for Crystal Structure Determinations, Siemens Industrial Automation Inc., Madison, MI, 1997.
40 B. E. Myers, L. Berger and S. A. Friedberg, *J. Appl. Phys.*, 1969, **40**, 1149.
41 G. Gliemann, *Theor. Chim. Acta*, 1962, **1**, 14.
42 R. G. Hayes, *J. Chem. Phys.*, 1966, **44**, 2210.